Simulation Study of Anti-Resonant Hollow Core Fibers for Beam-Driven THz-Applications

E. Gjonaj

gjonaj@temf.tu-darmstadt.de

TECHNISCHE UNIVERSITÄT DARMSTADT

DESY-TEMF Workshop

December 11, 2025, DESY, Hamburg

Outline

TECHNISCHE UNIVERSITÄT DARMSTADT

- Introduction & Motivation
- The waveguide mode problem
- The beam impedance problem
- ARF simulations
- Conclusions & Outlook

Introduction & Motivation

- Fundamentals of ARFs

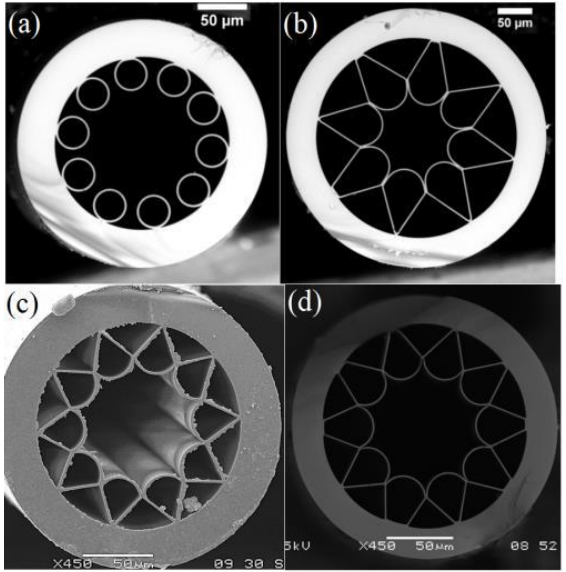

P. Jaworski, Sensors, 2021

- Hollow-core dielectric waveguides consisting of an outer cladding and various configurations of capillaries
- Strong field concentration in the core → low-losses in the cladding → low light attenuation
- Thin wall of capillary tubes acts as a Fabry-Perot resonator with:

$$\lambda_{res} = \frac{2t}{m}\sqrt{n_c^2 - 1}$$

$$\lambda_{antires} = \frac{4t}{2m+1}\sqrt{n_c^2 - 1}$$

t – capillary thickness
n_c – refraction index

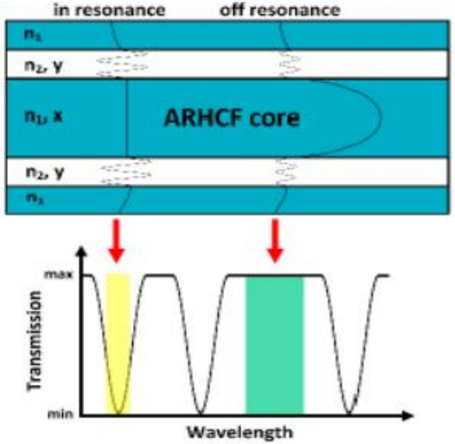

Introduction & Motivation

- Application of ARFs as beam-driven THz-source

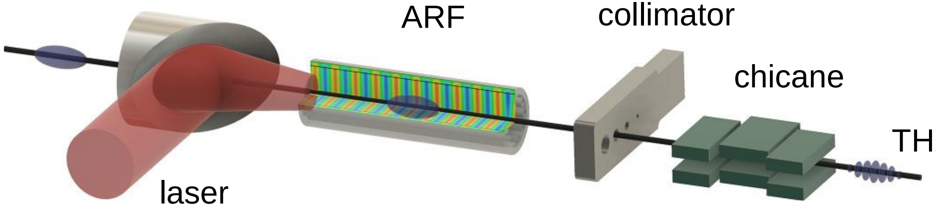

L. Genovese, et al., Phys. Rev. Res., 2023

Laser assisted density/energy modulation of a 100MeV electron bunch with a 2ps laser pulse

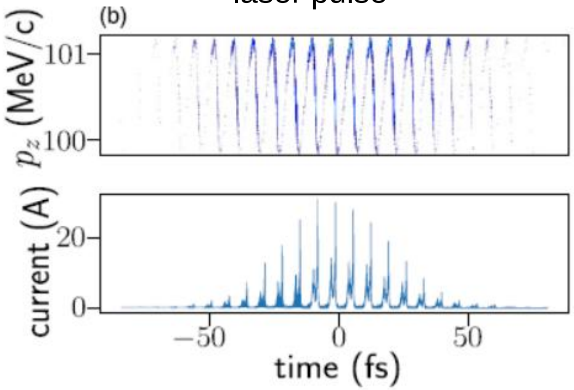

Goals of this study:

- Simulation method/tool for 2D dielectric, waveguide structures
- Investigate of the beam impedance in ARFs
- Incorporation of the impedance in beam dynamics simulations
- Optimization of the structure as a (passive or laser-driven) THz-source

Waveguide modes

- $\boldsymbol{E}_t$ - E_z - formulation for hybrid modes

$$\nabla \times \mu_r^{-1} \nabla \times \boldsymbol{E} - k_0^2 \varepsilon_r \boldsymbol{E} = 0$$

$$\underbrace{\boldsymbol{E} = \boldsymbol{E}_t + \hat{\boldsymbol{z}} E_z, \quad \nabla = \nabla_t + \hat{\boldsymbol{z}} j k_z}_{\text{transverse / longitudinal splitting}}$$

Transverse field equation:

$$\nabla_t \times \mu_r^{-1} \nabla_t \times \boldsymbol{E}_t + j k_z \mu_r^{-1} \nabla_t E_z + k_z^2 \mu_r^{-1} \boldsymbol{E}_t = k_0^2 \varepsilon_r \boldsymbol{E}_t$$

Longitudinal field equation: $-\nabla_t \mu_r^{-1} \nabla_t E_z + j k_z \nabla_t \cdot \mu_r^{-1} \boldsymbol{E}_t = k_0^2 \varepsilon_r E_z$

Generalized eigenvalue problem:

$$\begin{pmatrix} -\nabla_t \times \frac{1}{\mu_r} \nabla_t \times + k_0^2 \varepsilon_r & 0 \\ 0 & 0 \end{pmatrix} \begin{pmatrix} \boldsymbol{E}_t' \\ E_z' \end{pmatrix} = k_z^2 \begin{pmatrix} \frac{1}{\mu_r} & -\frac{1}{\mu_r} \nabla_t \\ \nabla_t \frac{1}{\mu_r} \cdot & -\nabla_t \frac{1}{\mu_r} \nabla_t - k_0^2 \varepsilon_r \end{pmatrix} \begin{pmatrix} \boldsymbol{E}_t' \\ E_z' \end{pmatrix} \qquad \left(\boldsymbol{E}_t = \frac{\boldsymbol{E}_t'}{k_z}, \; E_z = j E_z' \right)$$

Waveguide modes

- Finite element formulation

For each k_0^2, find $k_z^2 \in \mathbb{C}$ and $(\boldsymbol{e}_t, e_z) \in \mathbf{H}(curl, \Sigma) \times H^1(\Sigma)$ such that:

$$k_z^2\{(\mu_r^{-1}\boldsymbol{e}_t, \boldsymbol{\psi}_t) - (\mu_r^{-1}\nabla_t e_z, \boldsymbol{\psi}_t)\} = -(\mu_r^{-1}\nabla_t \times \boldsymbol{e}_t, \nabla_t \times \boldsymbol{\psi}_t) + k_0^2\,(\varepsilon_r \boldsymbol{e}_t, \boldsymbol{\psi}_t) \quad \forall \boldsymbol{\psi}_t \in \mathbf{H}(curl, \Sigma)$$

$$k_z^2\{(\mu_r^{-1}\nabla_t e_z, \nabla_t \phi) - k_0^2(\varepsilon_r e_z, \phi) - (\mu_r^{-1}\nabla_t \phi, \boldsymbol{e}_t)\} = 0 \quad \forall \phi \in H^1(\Sigma)$$

with boundary conditions:

PEC: $\begin{cases} \boldsymbol{n}_t \times \boldsymbol{e}_t = \boldsymbol{n}_t \times \boldsymbol{\psi}_t = 0 \\ e_z = \phi = 0 \end{cases}$ on $\partial\Sigma$

PMC: $\begin{cases} \boldsymbol{n}_t \cdot (\boldsymbol{\nabla}_t e_z + \boldsymbol{e}_t) = \cdots = 0 \\ \hat{\boldsymbol{z}} \cdot (\nabla_t \times \boldsymbol{e}_t) = \cdots 0 \end{cases}$ on $\partial\Sigma$

resulting in an algebraic eigenvalue problem

$$\begin{pmatrix} A_{11} & 0 \\ 0 & 0 \end{pmatrix} \begin{pmatrix} \boldsymbol{e}_t \\ e_z \end{pmatrix} = k_z^2 \begin{pmatrix} B_{11} & B_{12} \\ B_{12}^T & B_{22} \end{pmatrix} \begin{pmatrix} \boldsymbol{e}_t \\ e_z \end{pmatrix}$$

J.-F. Lee, et al., IEEE Trans. MTT, 1991

Waveguide modes

- ARF geometry & mesh

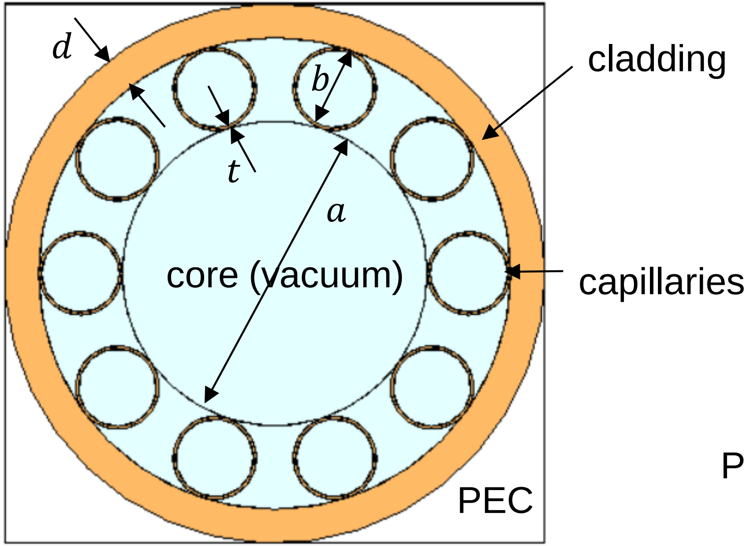

L. Genovese, et al., Phys. Rev. Res., 2023

$a/\mu m$	$b/\mu m$	$d/\mu m$	$t/\mu m$	ε_r
157	40	35	1.5	3.8

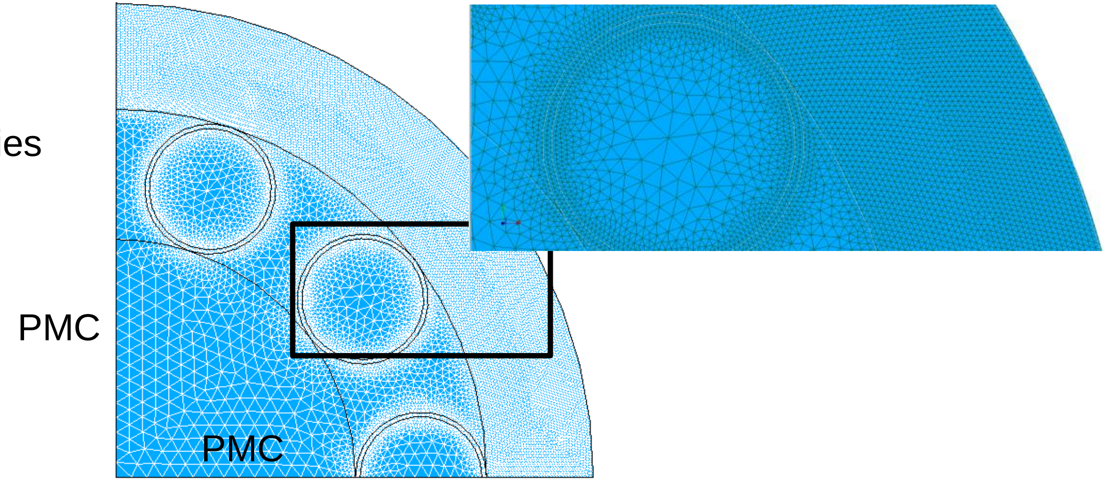

Waveguide modes

- Dispersion curves

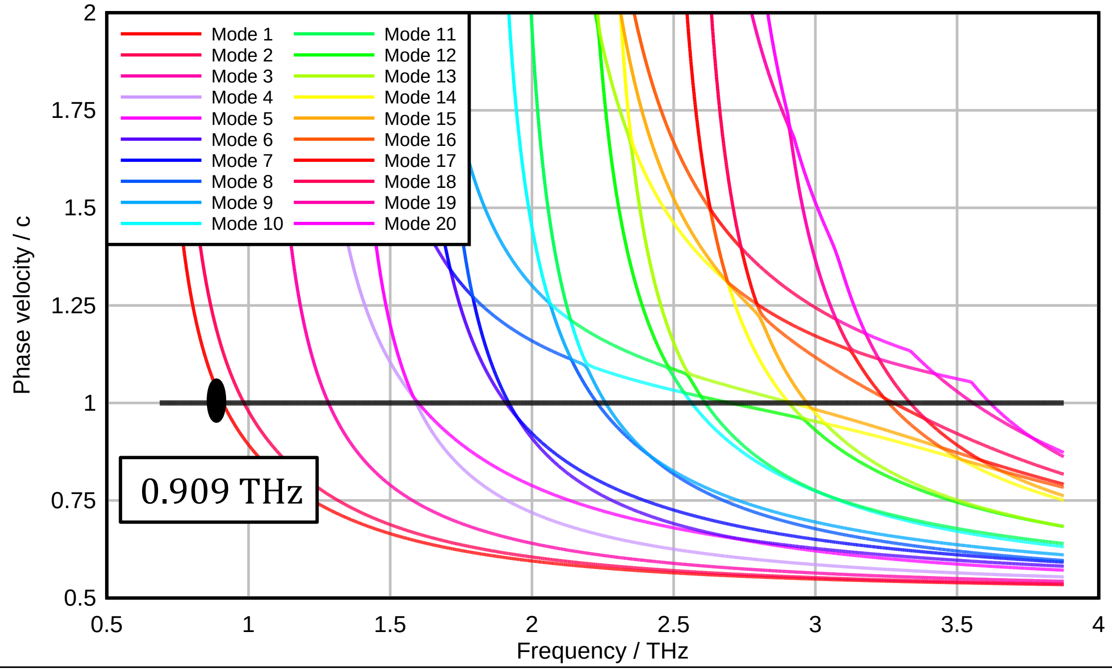

Mode #1 @0.909 THz

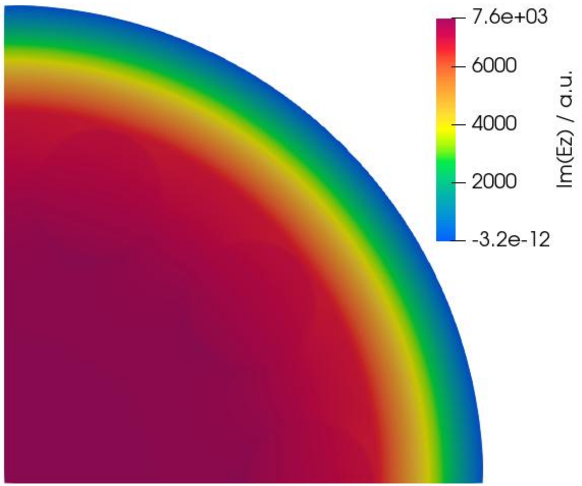

Waveguide modes

- Dispersion curves

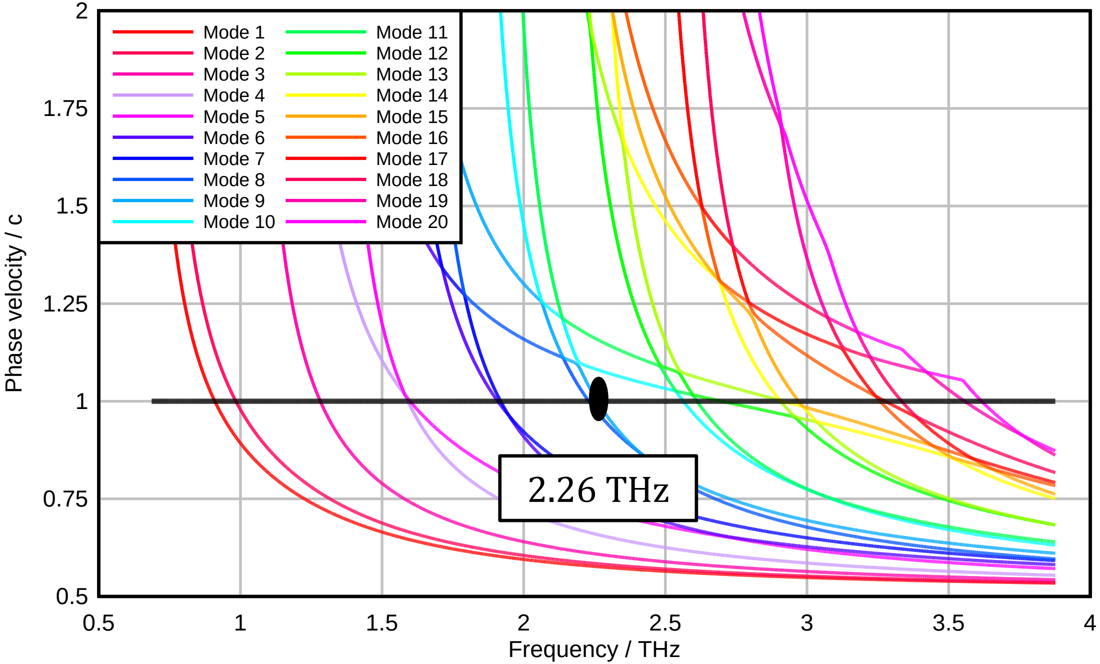

Mode #9 @2.26 THz

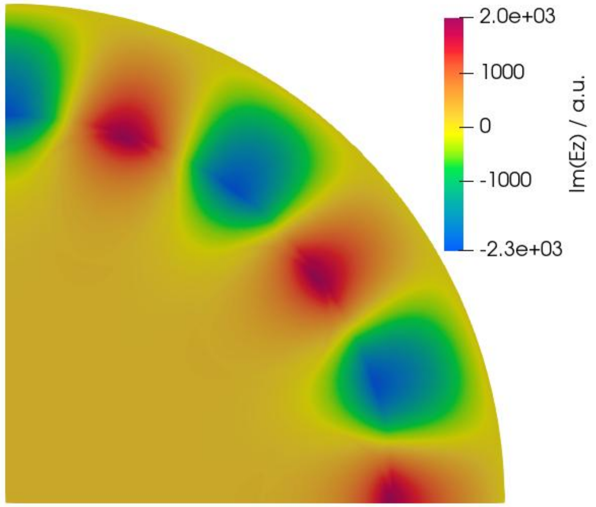

Waveguide modes

- Dispersion curves

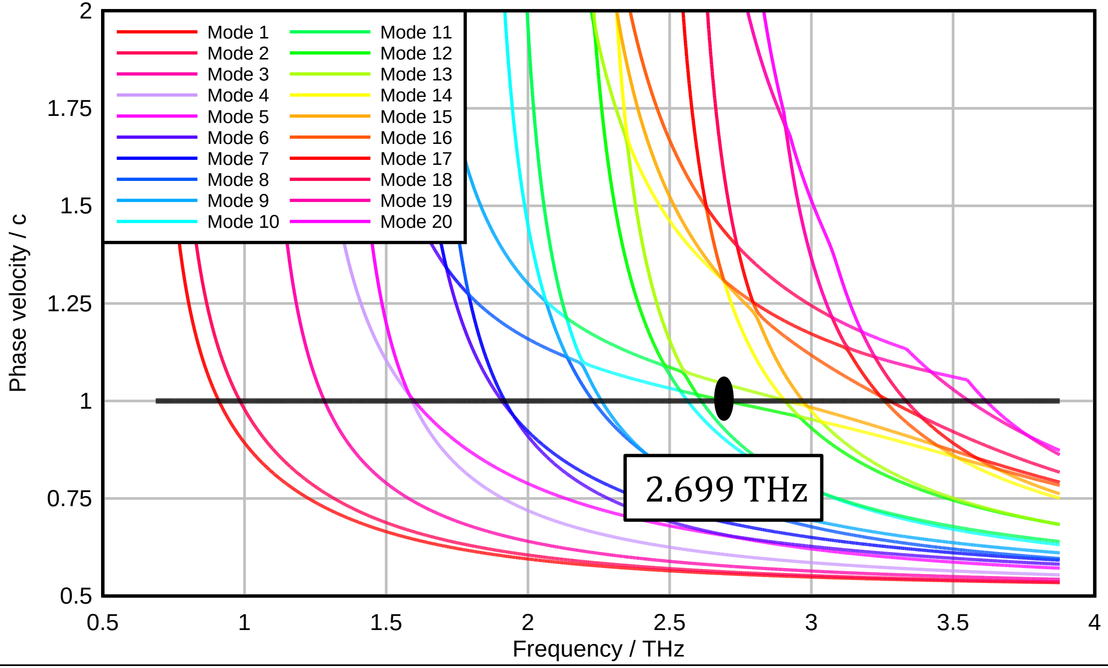

Mode #12 @2.699 THz

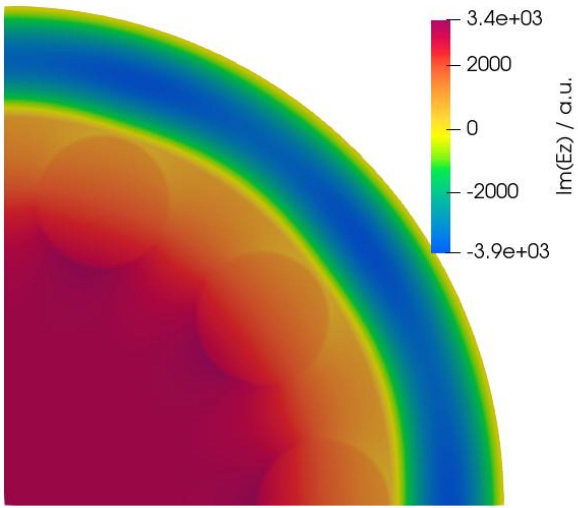

Waveguide modes

- Comparison with CST

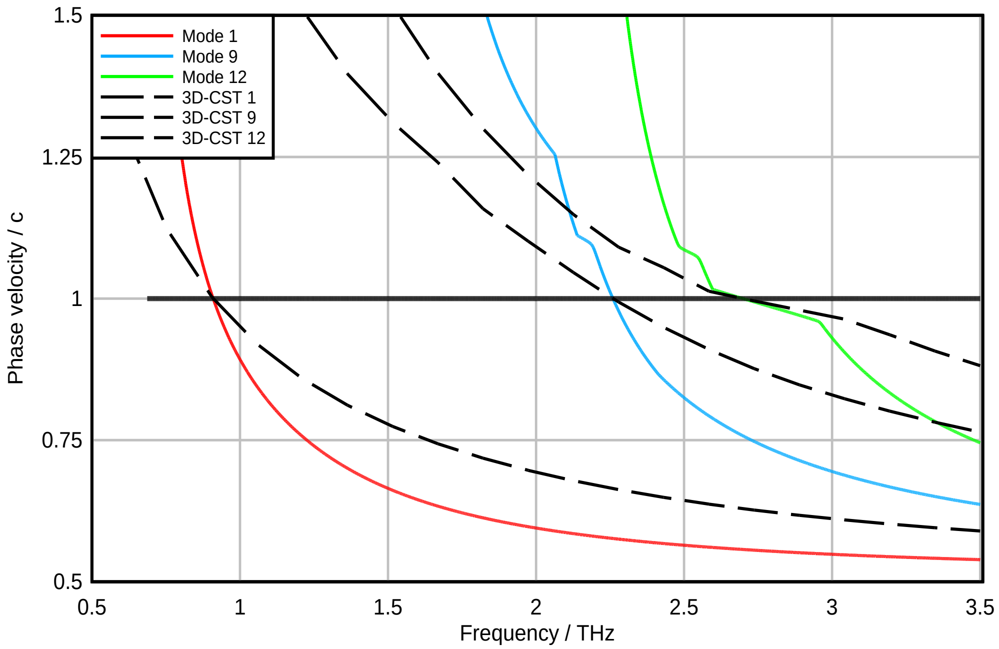

3D-CST eigenmode solver with periodic BC

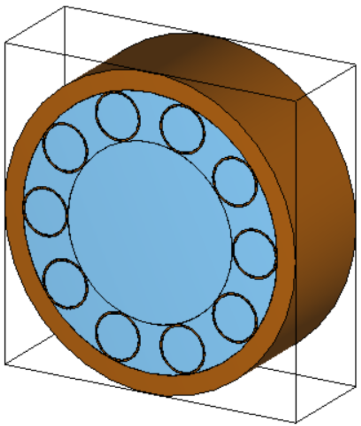

Synchronous mode frequencies / THz

#	2D	3D-CST
1	0.909	0.909
9	2.260	2.261
12	2.699	2.70

The beam impedance problem

- Equations

$$\begin{pmatrix} \frac{1}{k_z^2}\nabla_t \times \frac{1}{\mu_r}\nabla_t \times -\frac{k_0^2}{k_z^2}\varepsilon_r + \frac{1}{\mu_r} & -\frac{1}{\mu_r}\nabla_t \\ \nabla_t \frac{1}{\mu_r}\cdot & -\nabla_t \frac{1}{\mu_r}\nabla_t - k_0^2\,\varepsilon_r \end{pmatrix} \begin{pmatrix} \boldsymbol{E}_t' \\ E_z' \end{pmatrix} = \begin{pmatrix} 0 \\ k_0 Z_0 J_z \end{pmatrix}$$

$$k_z = \frac{\omega}{c\beta_z}$$

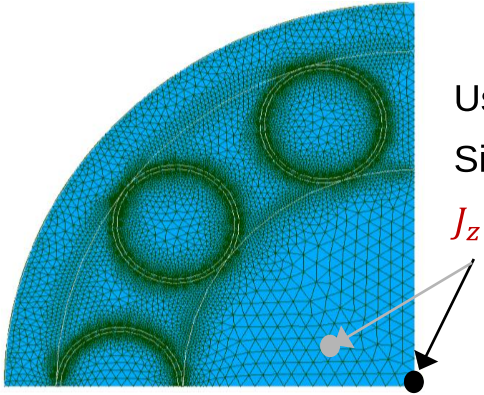

Using the same matrix operators as before

Single or multiple source/test node excitation:

$J_z(r,\omega) = q_0\delta(r - r_0)$

Similar (but not identical) formulation in:

B. Doliva, et al., PAC 2005
U. Niedermayer, et al., PR-STAB, 2015

The beam impedance problem

- Validation

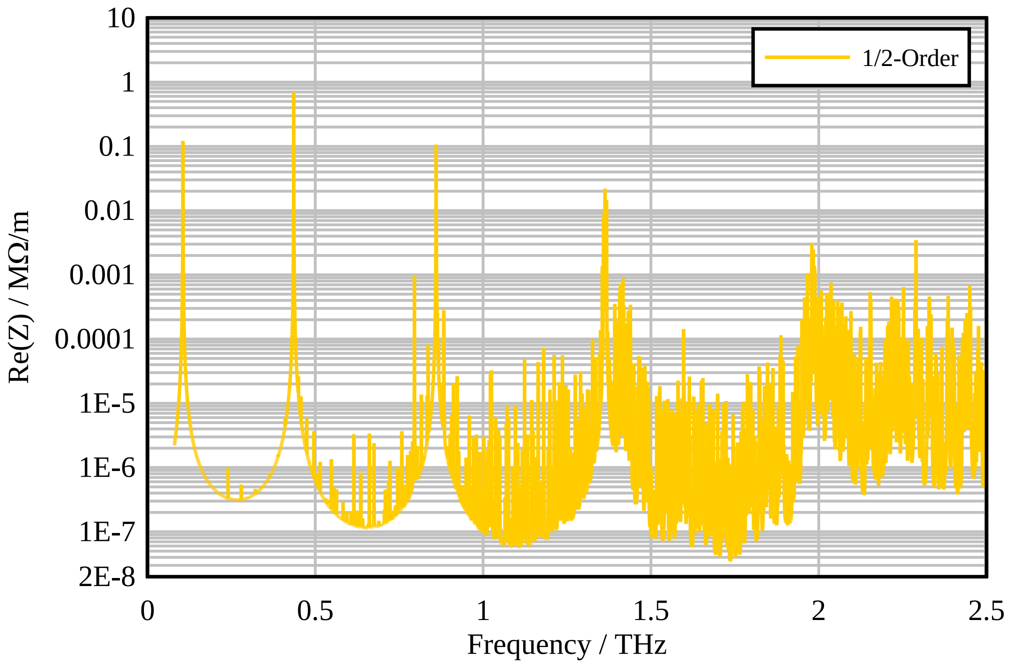

Two-layer, dielectric loaded pipe

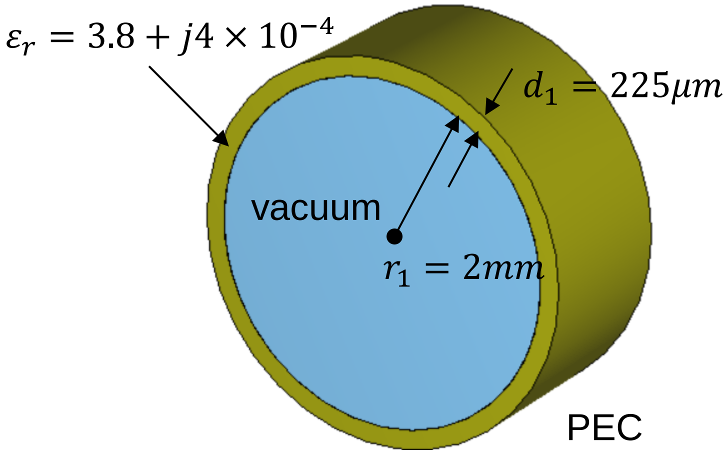

K. Floettmann, et al., J. Synch. Rad., 2020

Ivanyan et al., PR-STAB, 2008

The beam impedance problem

- Validation

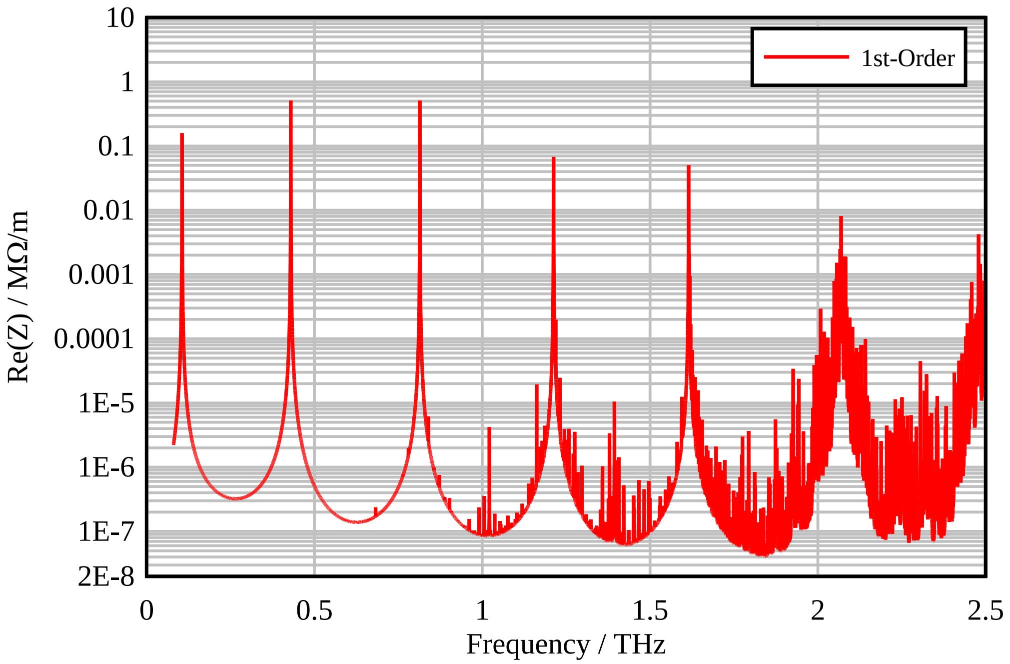

Two-layer, dielectric loaded pipe

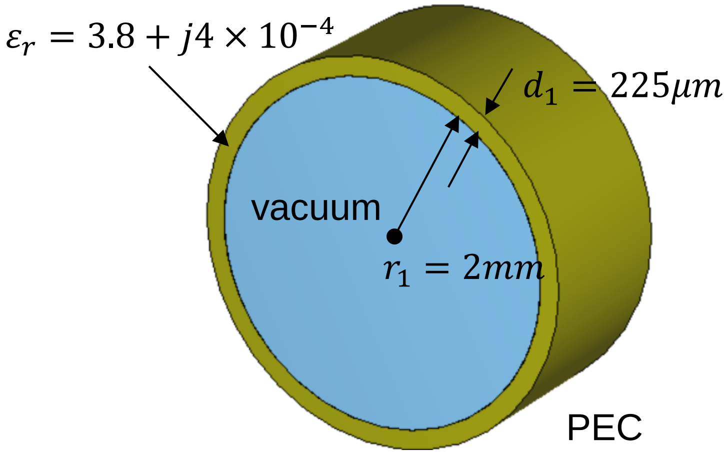

K. Floettmann, et al., J. Synch. Rad., 2020

Ivanyan et al., PR-STAB, 2008

The beam impedance problem

- Validation

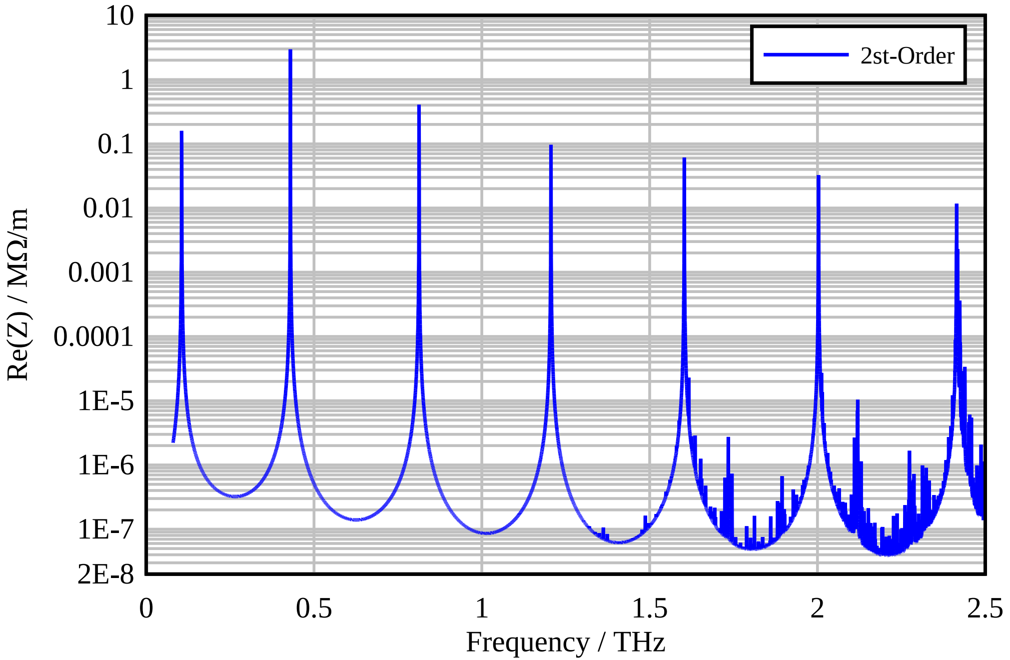

Two-layer, dielectric loaded pipe

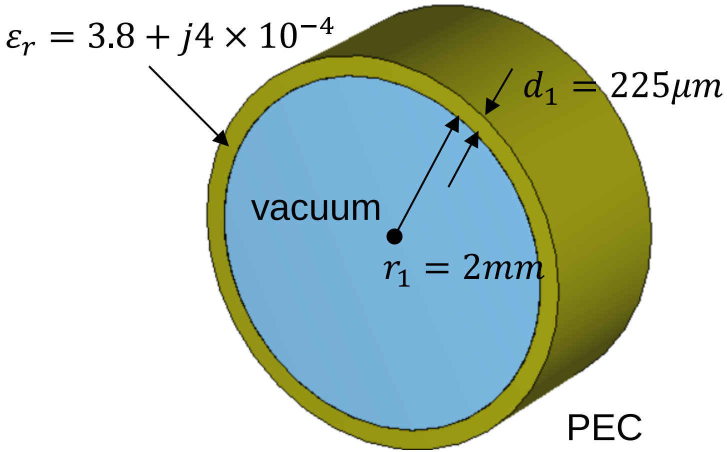

K. Floettmann, et al., J. Synch. Rad., 2020

Ivanyan et al., PR-STAB, 2008

The beam impedance problem

- Validation

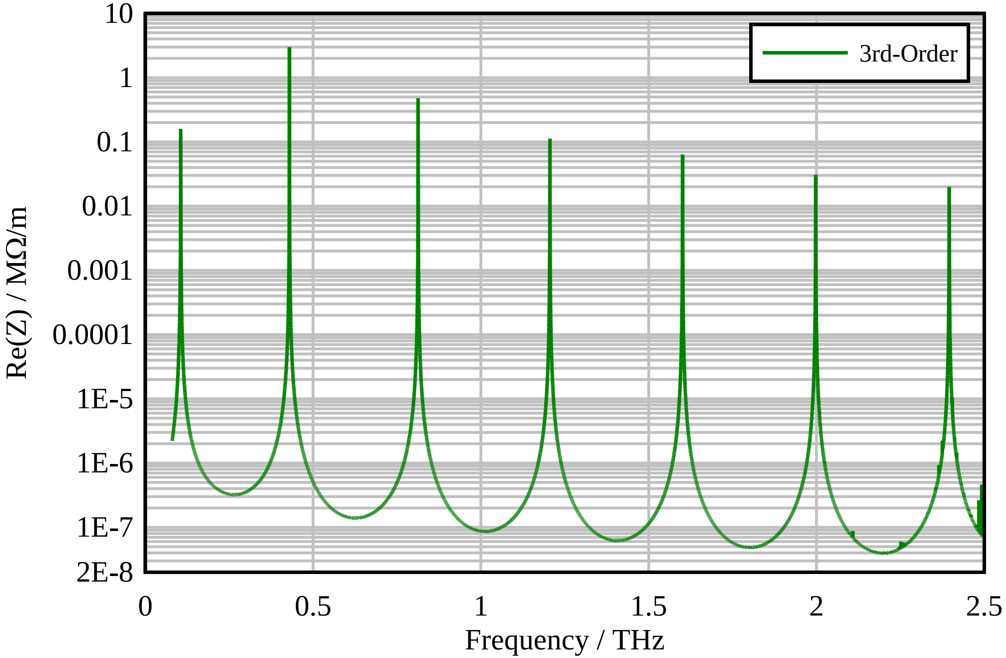

Two-layer, dielectric loaded pipe

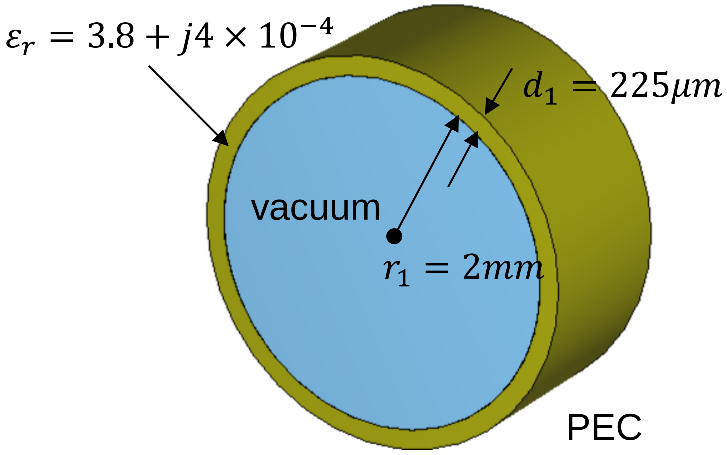

K. Floettmann, et al., J. Synch. Rad., 2020

Ivanyan et al., PR-STAB, 2008

The beam impedance problem

- Validation

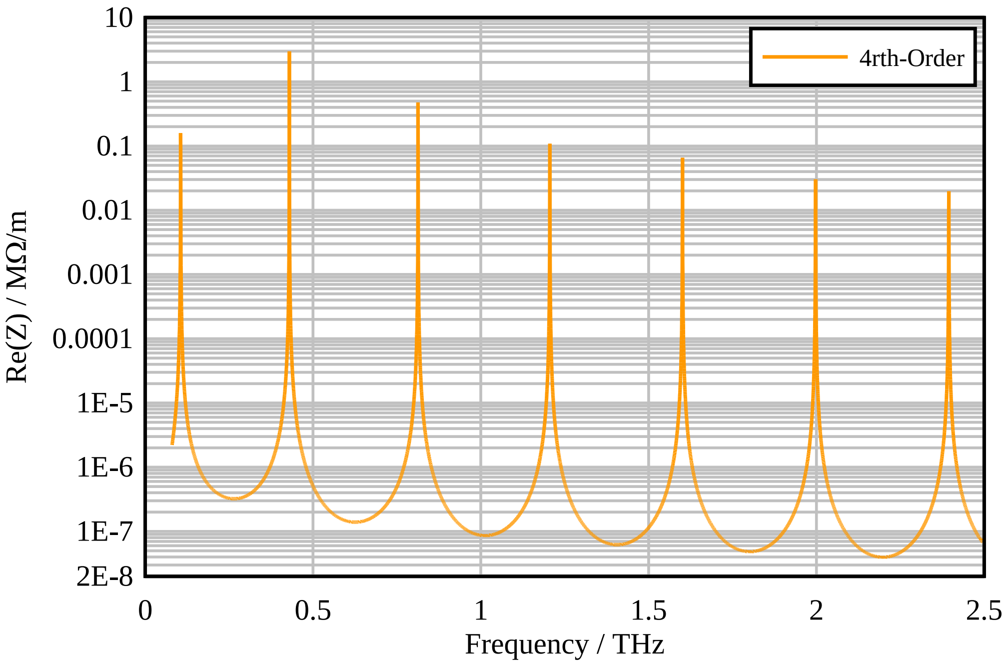

Two-layer, dielectric loaded pipe

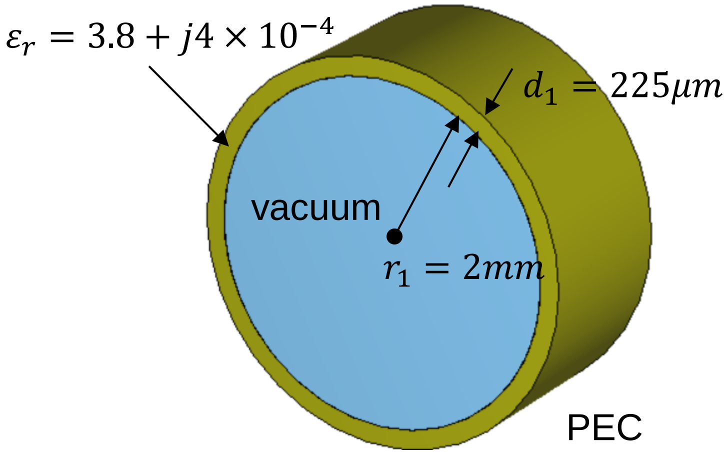

K. Floettmann, et al., J. Synch. Rad., 2020
Ivanyan et al., PR-STAB, 2008

The beam impedance problem

- Validation

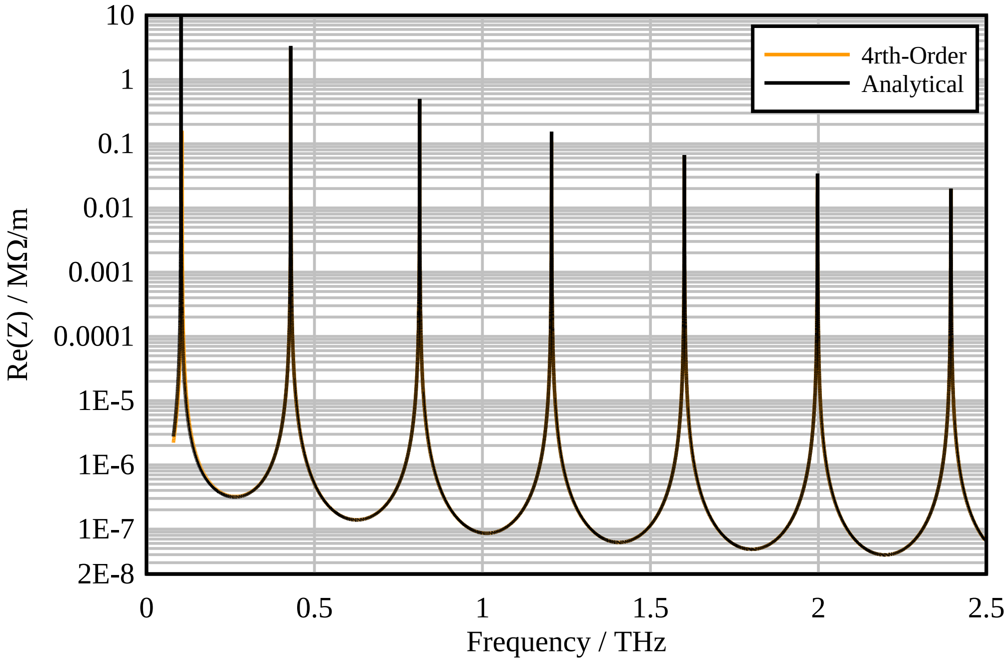

Two-layer, dielectric loaded pipe

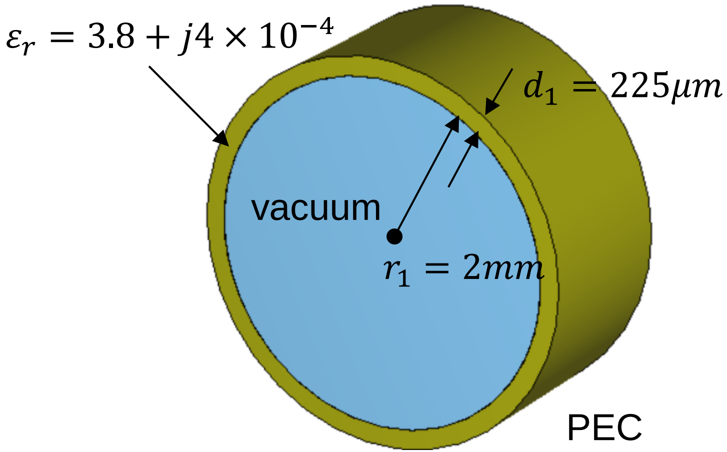

K. Floettmann, et al., J. Synch. Rad., 2020

Ivanyan et al., PR-STAB, 2008

The beam impedance problem

- Validation

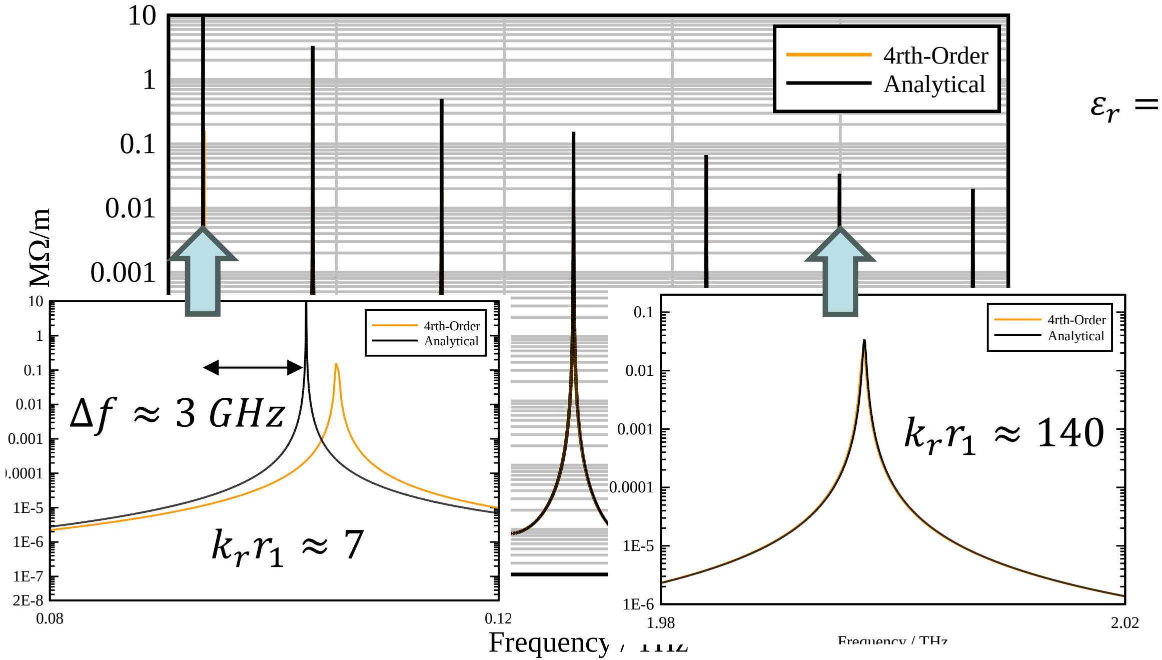

Two-layer, dielectric loaded pipe

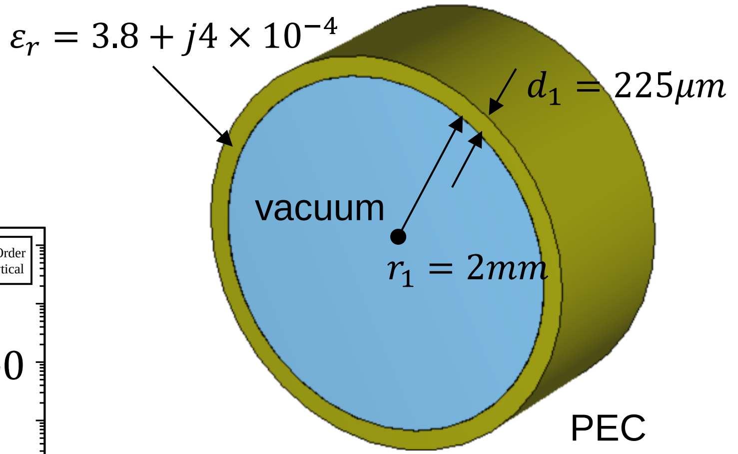

K. Floettmann, et al., J. Synch. Rad., 2020

Ivanyan et al., PR-STAB, 2008

The beam impedance problem

- Comparison with CST (ground mode)

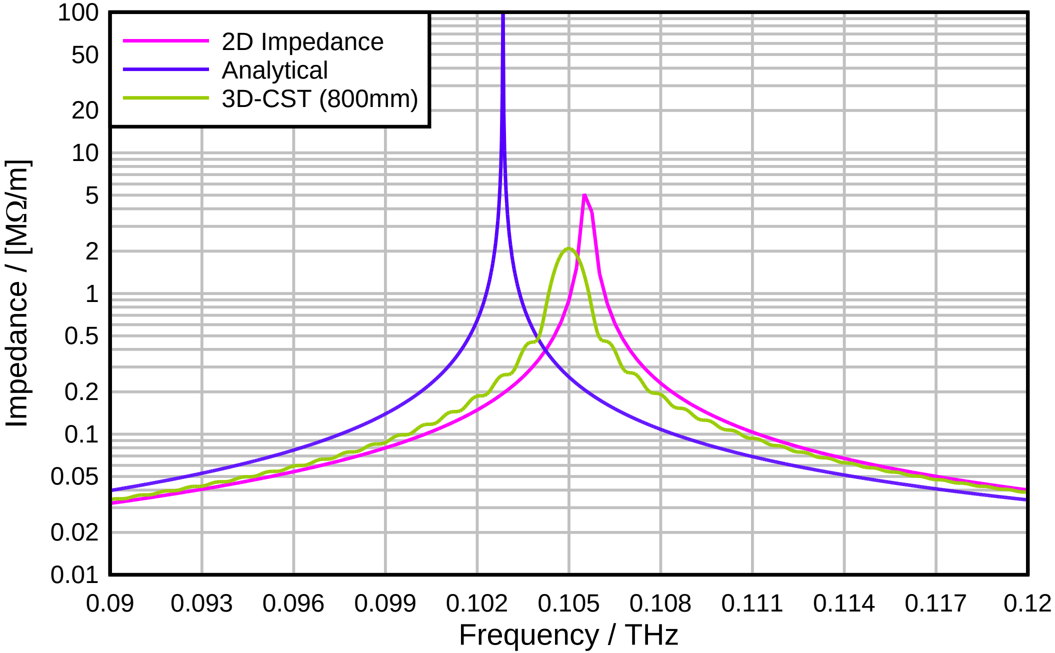

Two-layer, dielectric loaded pipe

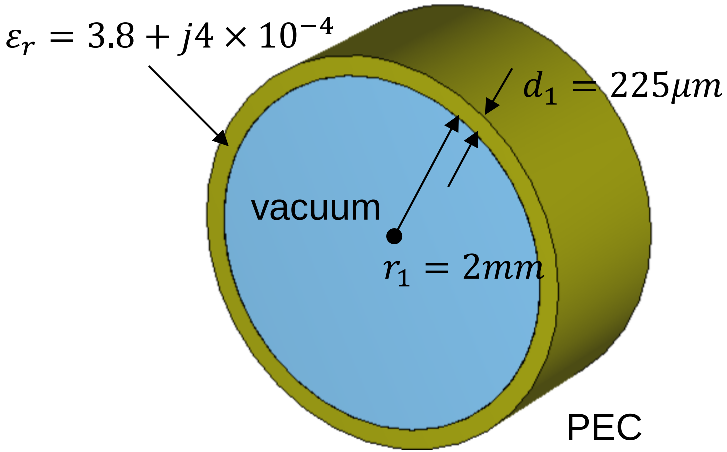

K. Floettmann, et al., J. Synch. Rad., 2020

Ivanyan et al., PR-STAB, 2008

ARF impedance

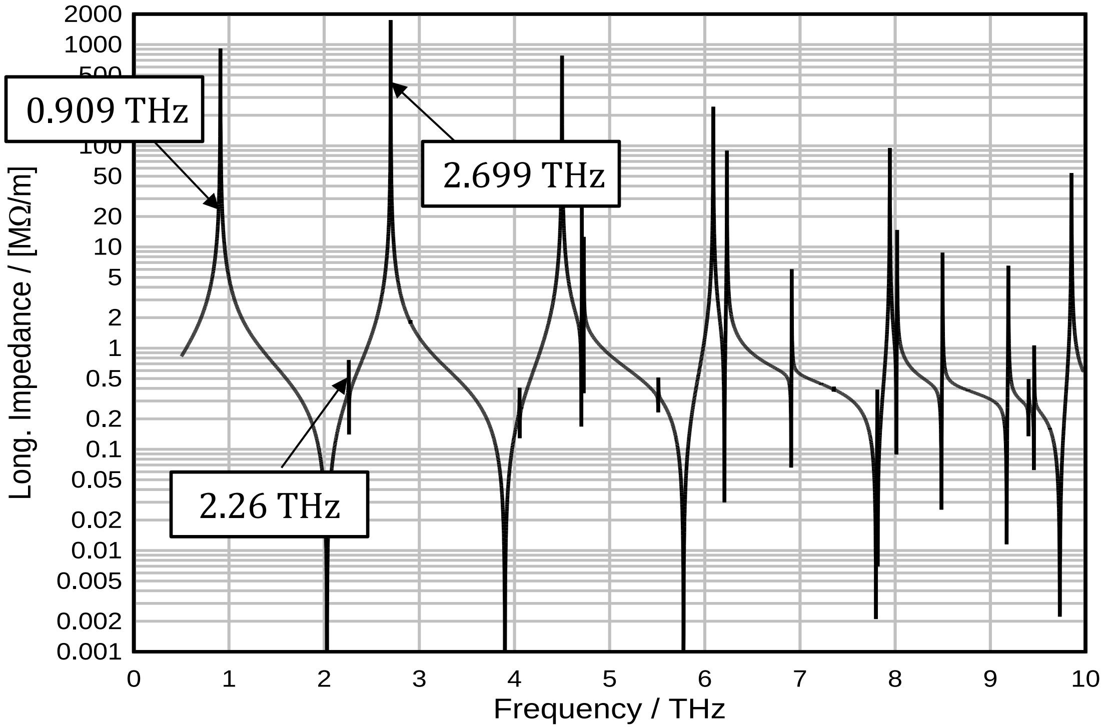

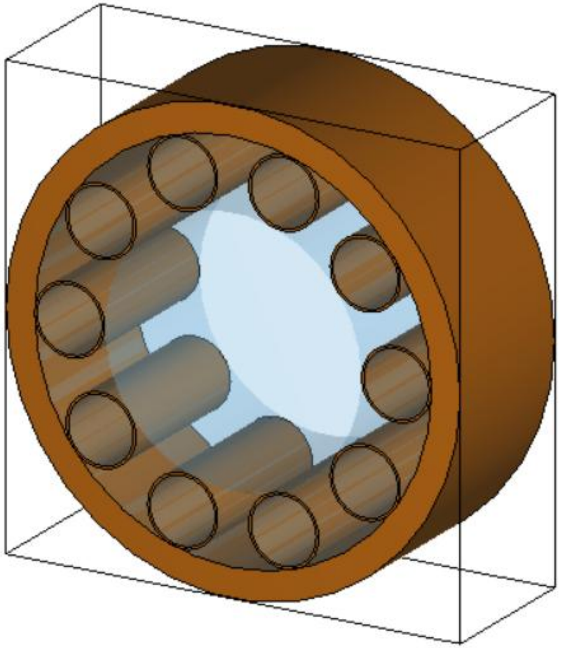

ARF impedance

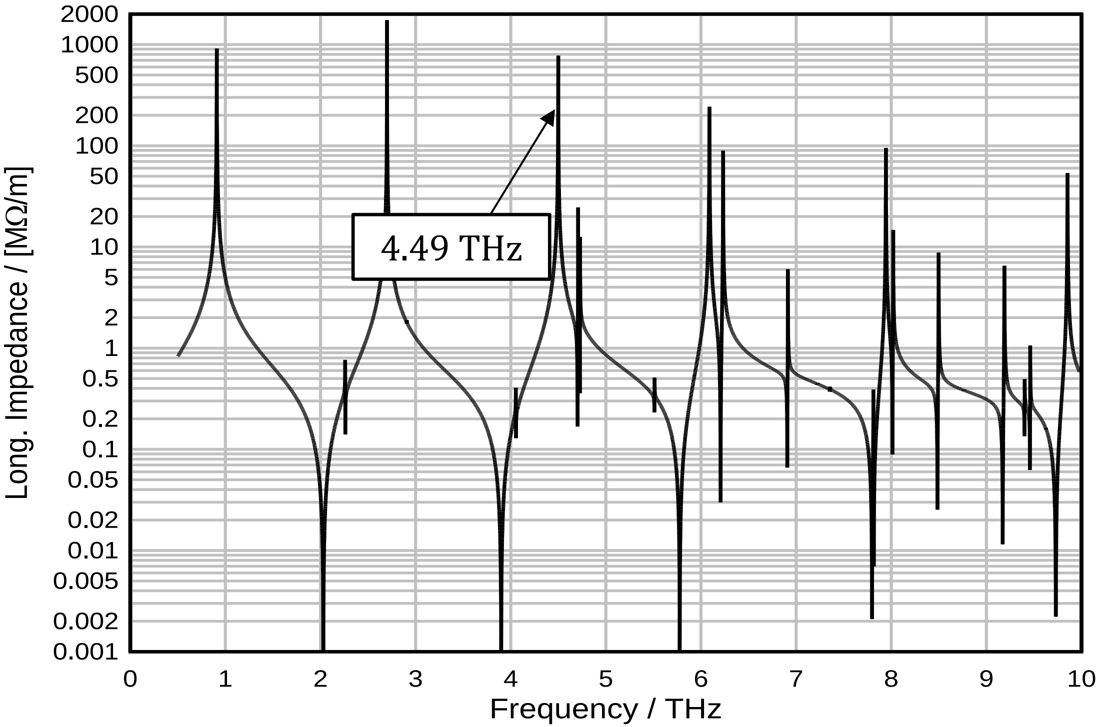

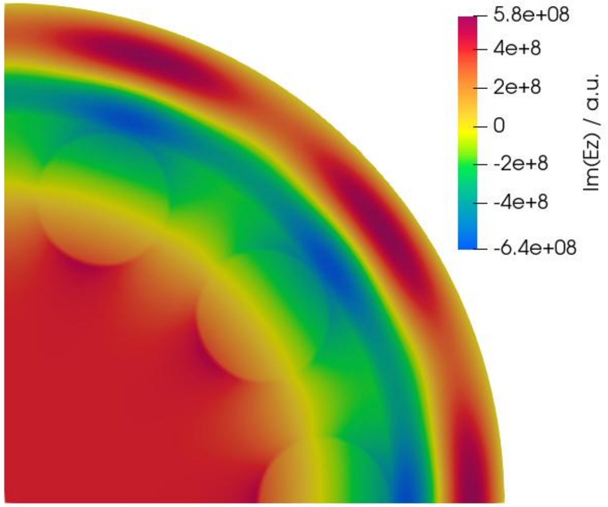

ARF impedance

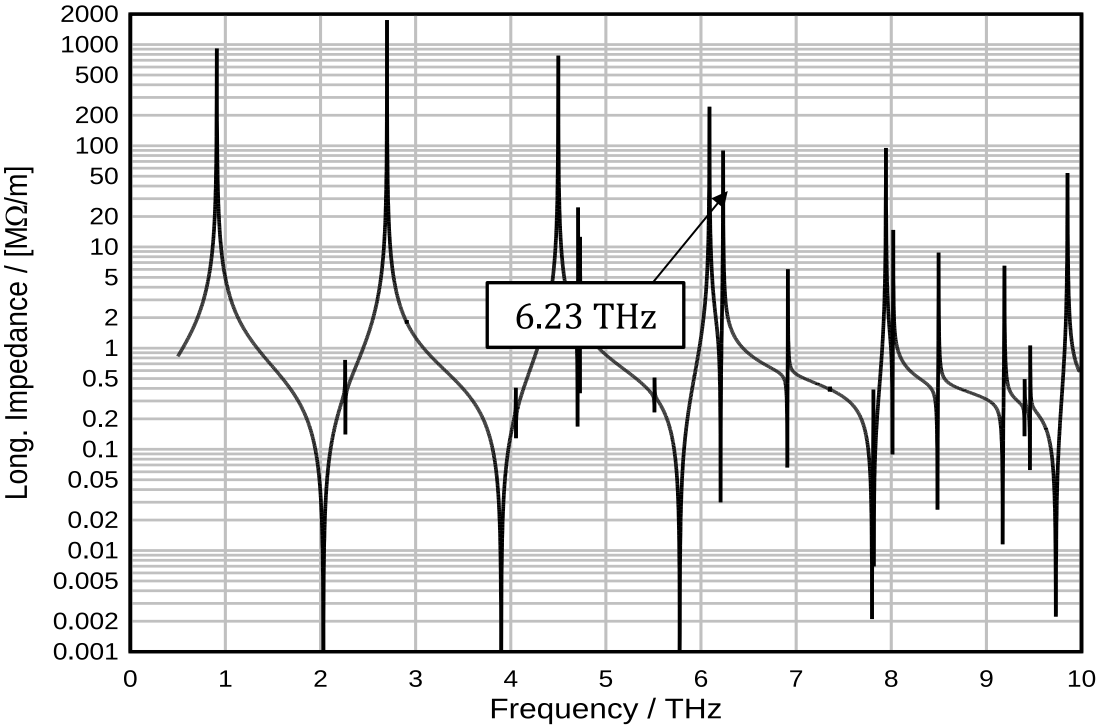

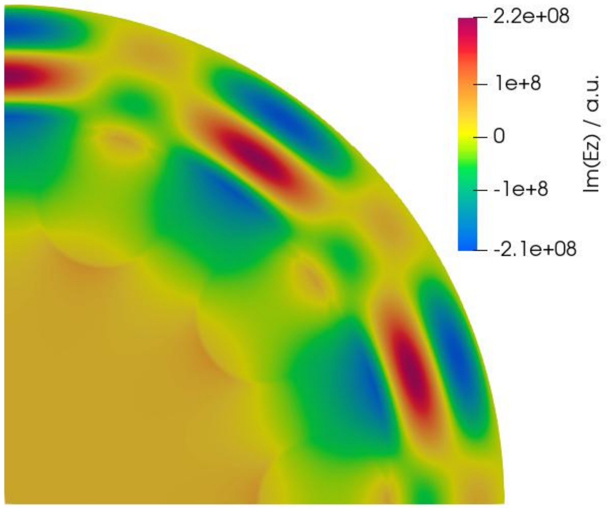

ARF impedance

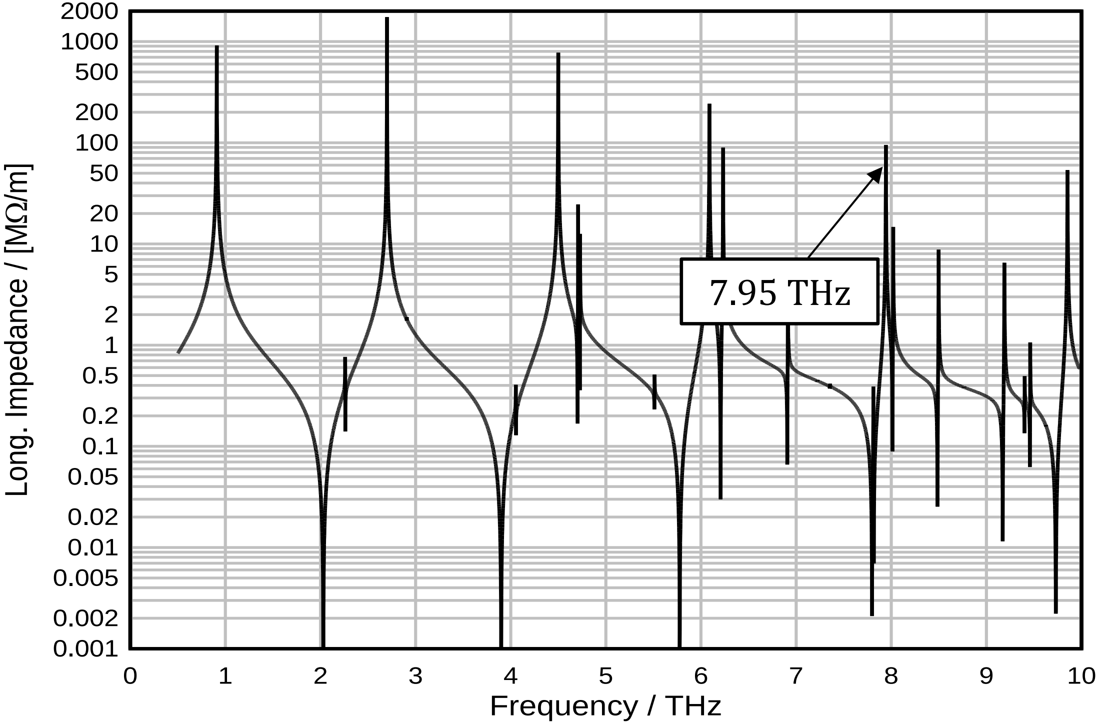

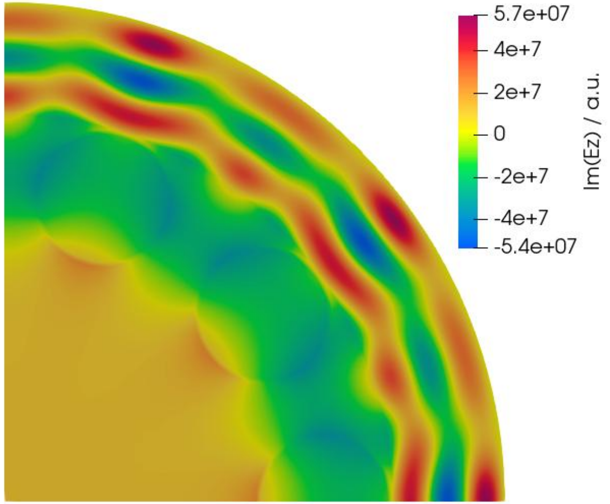

ARF impedance

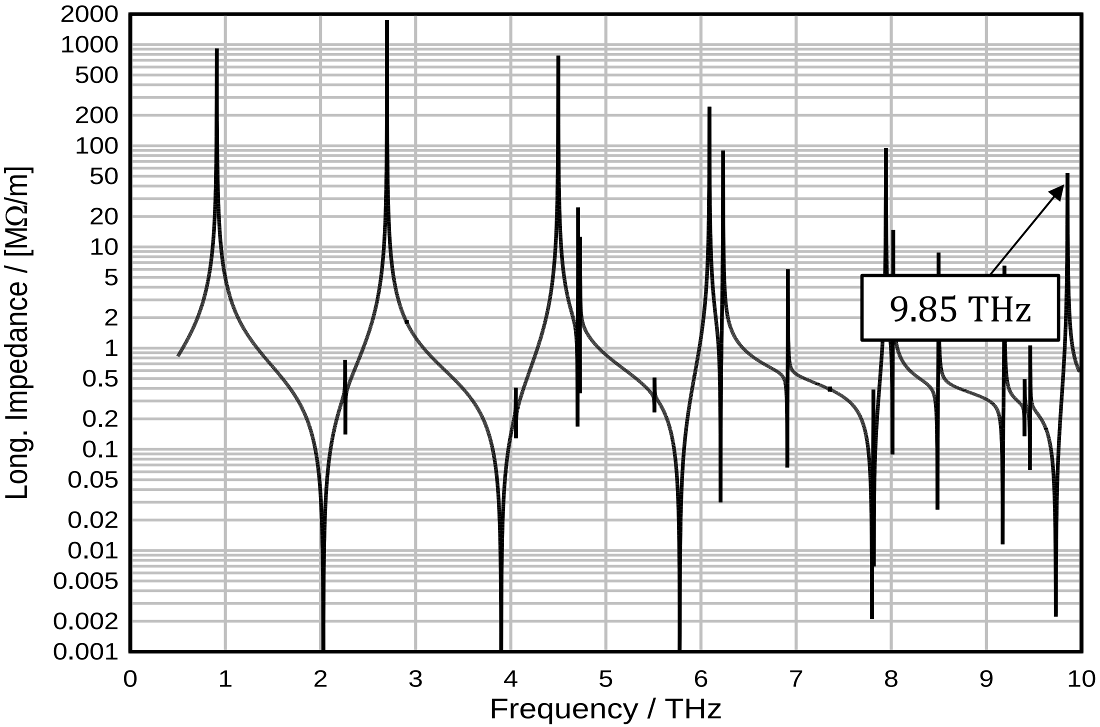

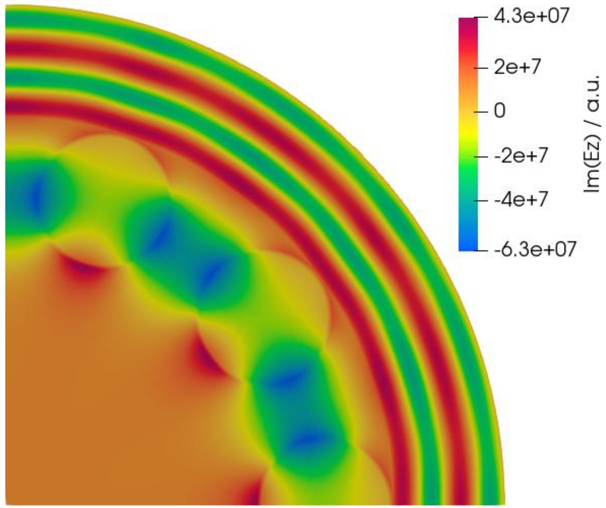

ARF impedance

- (Anti-) resonance condition

$$\lambda_{antires} = \frac{4t}{2m+1}\sqrt{n_c^2 - 1} \quad \rightarrow \quad f_{antires} \approx 0.45 \cdot 10^8 \frac{2m+1}{t} \text{ [Hz]}, \qquad \rightarrow \quad f_{antires}\,(0,1) = \{30,90\} \text{ THz}$$

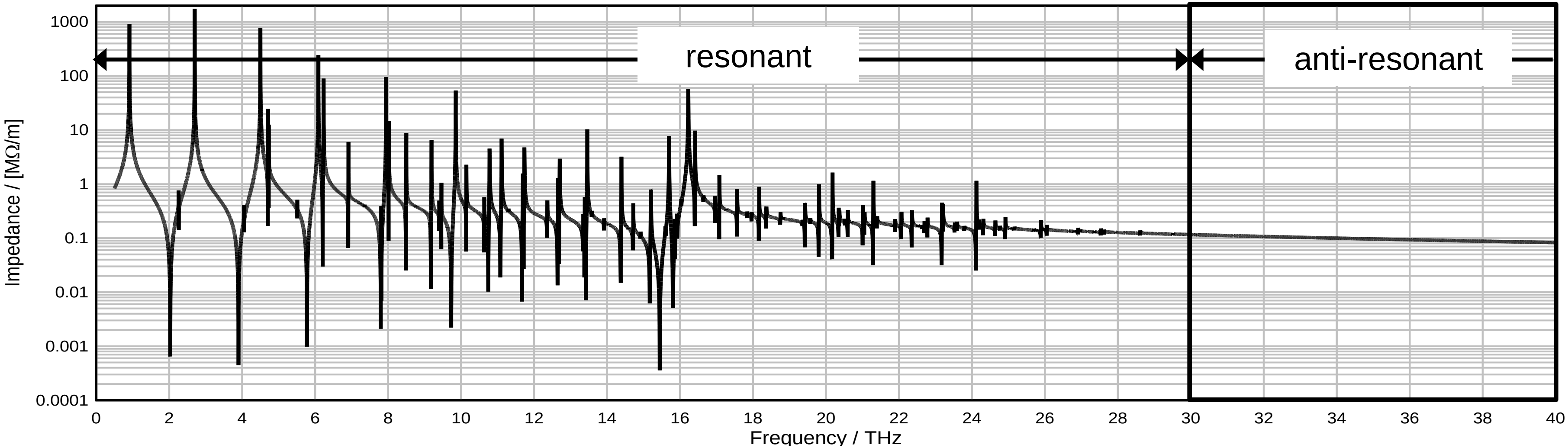

ARF impedance

- (Anti-) resonance condition

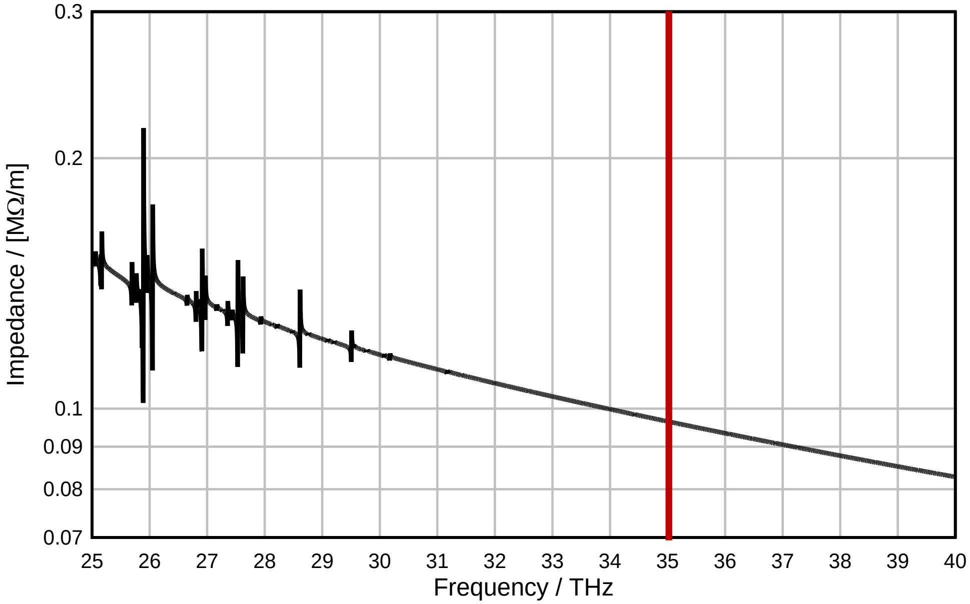

Longitudinal field pattern at 35 THz

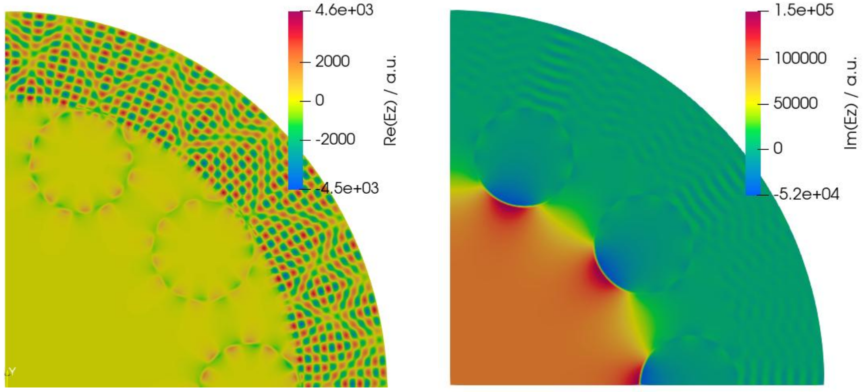

ARF impedance

Field pattern at 35 THz

- (Anti-) resonance condition

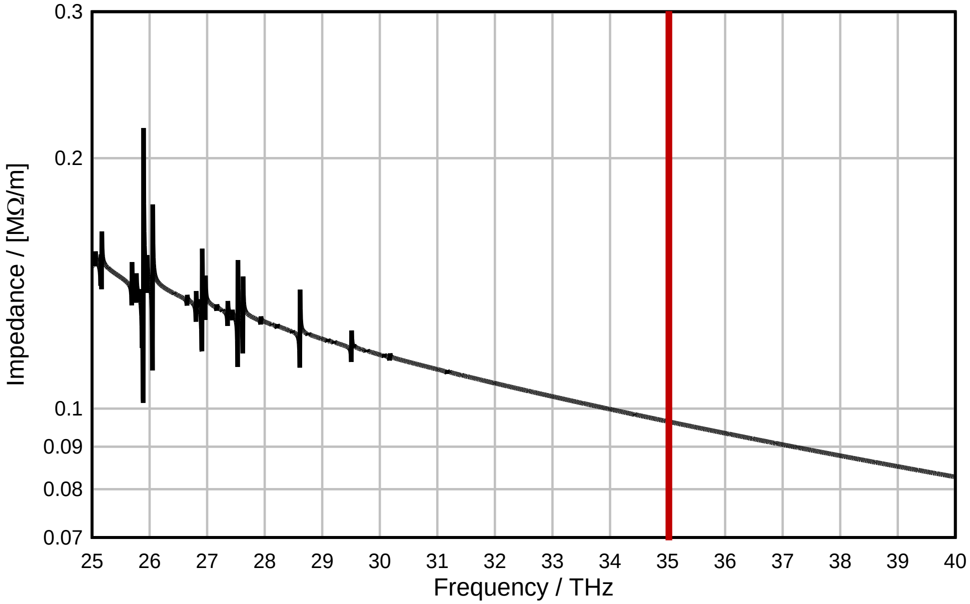

Longitudinal field pattern at 35 THz

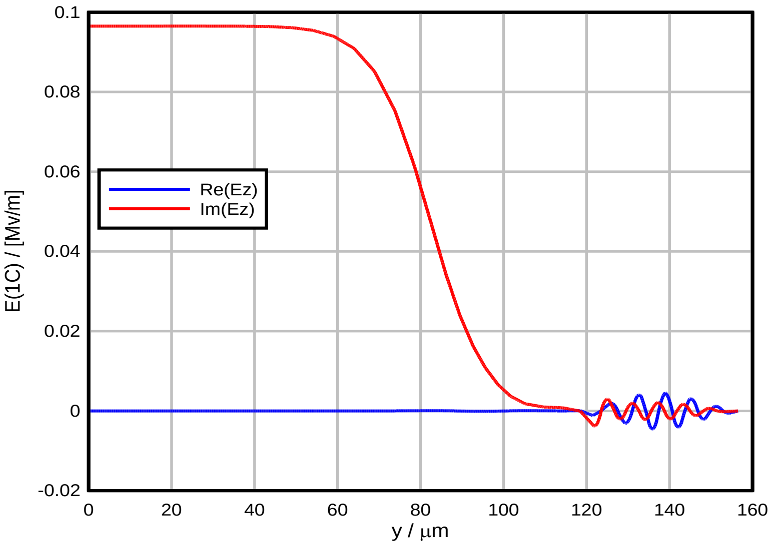

Summary & Conclusions

- 2D-simulation code for the computation of dielectric waveguides
  - High-order conforming FEM on curved elements for accurate geometry approximation
  - **Analysis of hybrid waveguide modes**
  - **Computation of the beam coupling impedance**
  - Validation shows excellent agreement with analytical solutions and 3D-CST
- Simulation of ARFs for beam driven THz-source
  - Multiple impedance resonances in the ARFs resonant frequency range, but no obvious “field confinement” effect
  - Field confinement in the core under anti-resonant conditions, however, very weak coupling to the beam
  - We still need to consider the effect of frequency dependent dielectric losses, finite length of the fibers and, eventually, longitudinally periodic ARFs

ARF impedance

- Perfectly round fiber with thin inner layer

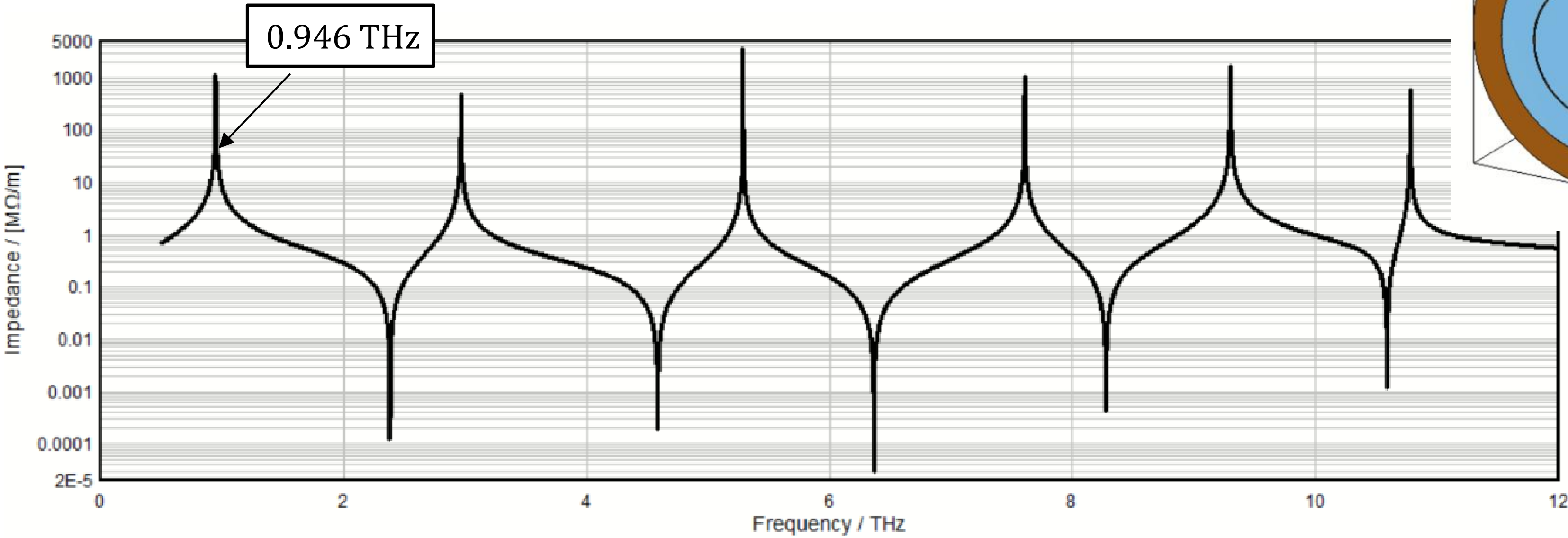

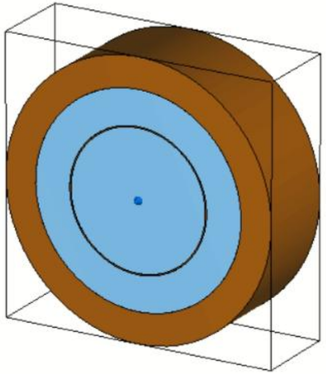

ARF impedance

- Perfectly round fiber with thin inner layer

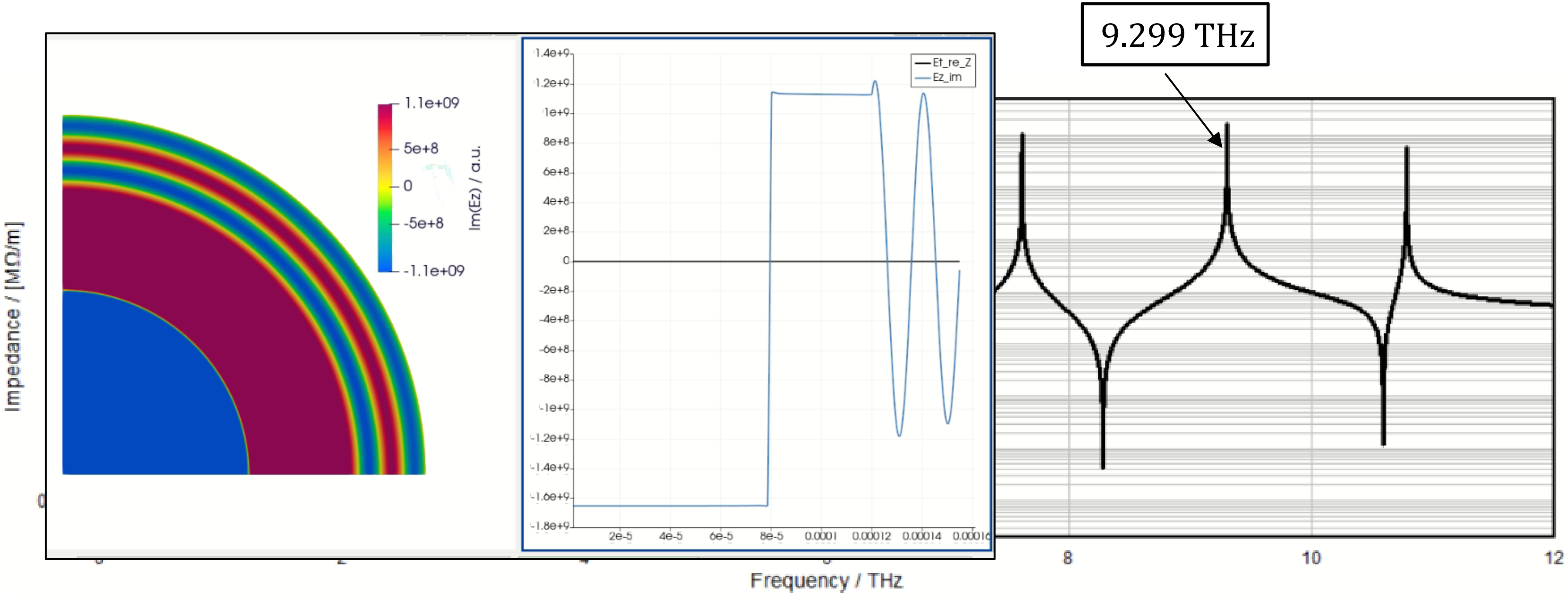

ARF impedance

- Perfectly round fiber with thin inner layer

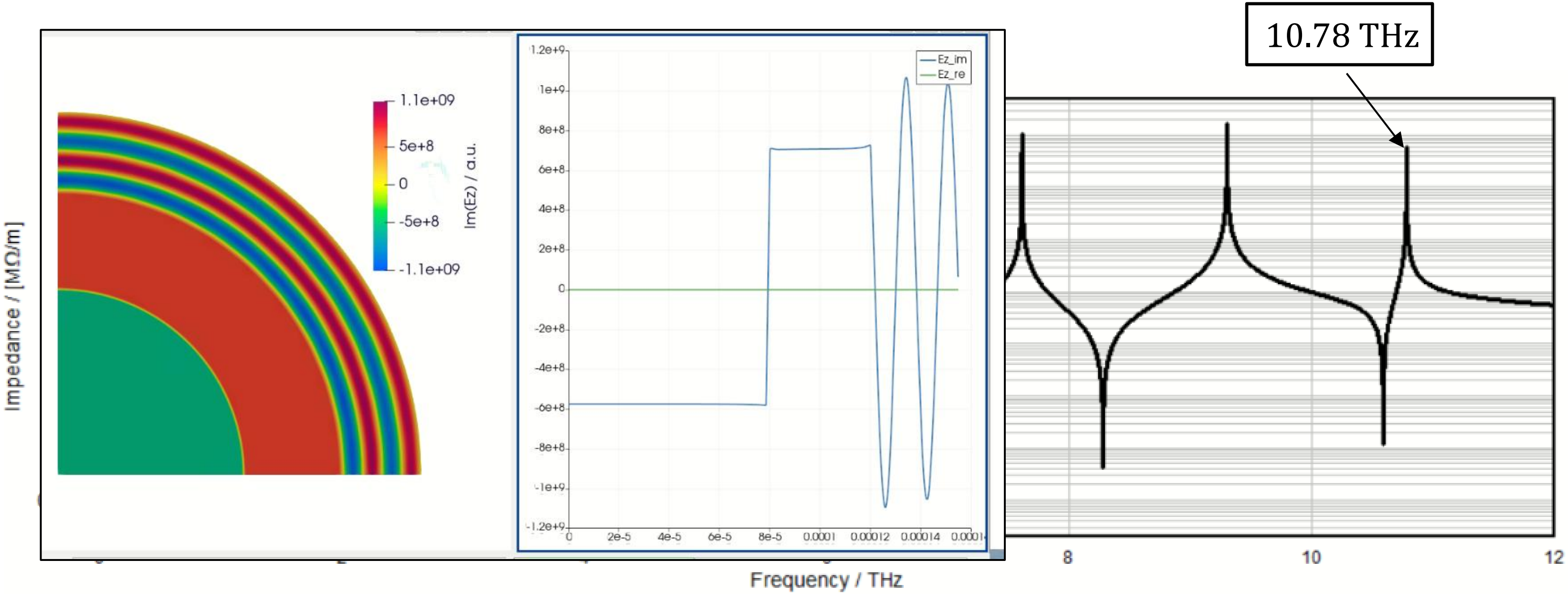

ARF impedance

- Perfectly round fiber with thin inner layer